

# Inverse Chiral Phonon Zeeman Effect in Noncentrosymmetric Crystals

Jun-ichiro Kishine,<sup>1,2</sup> A. S. Ovchinnikov,<sup>3,4</sup> Masahiro Sato,<sup>5</sup> G. N. Makarov,<sup>6,7</sup> and A. D. Lyakhov<sup>4</sup>

<sup>1</sup>*Division of Natural and Environmental Sciences,*

*The Open University of Japan, Chiba 261-8586, Japan*

<sup>2</sup>*Quantum Research Center for Chirality, Institute for Molecular Science, Okazaki, Aichi 444-8585, Japan*

<sup>3</sup>*M.N. Mikheev Institute of Metal Physics, Ural Division,*

*Russian Academy of Sciences, Ekaterinburg 620219, Russia*

<sup>4</sup>*Institute of Natural Science and Mathematics, Ural Federal University, Ekaterinburg 620002, Russia*

<sup>5</sup>*Department of Physics, Chiba University, Chiba 263-8522, Japan*

<sup>6</sup>*Landau Institute for Theoretical Physics, Chernogolovka 142432, Russia*

<sup>7</sup>*Moscow Institute of Physics and Technology, Dolgoprudnyi 141700, Russia*

(Dated: January 21, 2026)

We present a microscopic theory of the inverse chiral phonon Zeeman effect in noncentrosymmetric crystals. Within micropolar elasticity, coupled translational displacements and microrotations give rise to intrinsically chiral phonons, which generate an elliptically polarized internal magnetic field through dynamical piezoelectricity. In the high-frequency Floquet regime and under incomplete electronic screening, this field acts as an effective longitudinal Zeeman field on electronic spins, leading to spin polarization and band splitting. The results establish a purely lattice-driven mechanism for the inverse chiral phonon Zeeman effect in noncentrosymmetric crystals.

The magnetic activity of lattice vibrations was already recognized in the 1970s by pioneering Raman studies of rare-earth compounds [1, 2]. In recent years, this long-standing concept has been revitalized by modern spectroscopic techniques, which revealed that circularly polarized (axial) phonons can carry angular momentum and induce magnetization even in nonmagnetic solids [3–7]. The associated phonon magnetic moments are now known to reach values comparable to several Bohr magnetons, establishing a rapidly growing research field on phono-magnetic effects [8].

This family of phenomena is collectively referred to as the *phonon Zeeman effect*, where an external magnetic field lifts the degeneracy of two orthogonal optical phonon modes and produces right- and left-handed branches. Giant phonon magnetic moments—comparable to several  $\mu_B$ —have been experimentally identified in some compounds [9–12]. These observations provide quantitative evidence that lattice dynamics, assisted by electron–phonon coupling, can generate effective magnetic responses far beyond the nuclear-magneton scale.

The inverse process—in which lattice motion itself generates magnetization rather than responding to it—is known as the *inverse phonon Zeeman effect*. Its microscopic origin has been discussed in terms of the *phonon inverse Faraday effect* or *dynamical multiferroicity* [3, 5, 7, 13–16], where a time-dependent polarization  $\mathbf{P}(t)$  induces magnetization  $\mathbf{M} \sim \mathbf{P} \times \dot{\mathbf{P}}$  [3, 5]. Within a Landau-type phenomenological description, the resulting magnetization is proportional to the imbalance between right- and left-handed phonon amplitudes [8, 15]. The phonon-induced magnetic response has also been interpreted as a pseudofield [17, 18].

From this viewpoint, focusing on noncentrosymmetric crystals—where the degeneracy between left- and

right-handed vibrational modes is lifted from the outset—naturally suggests an enhanced internal magnetic response. In particular, crystals with helical or screw-axis symmetries intrinsically lift the degeneracy between phonons of opposite helicities, giving rise to truly chiral phonons [19], while lattice deformations are generically coupled to electric polarization via the piezoelectric effect. In this context, the present work goes beyond descriptions based on merely rotating (axial) phonon modes and instead elevates the framework to truly chiral phonons, in which rotational and translational lattice dynamics are intrinsically intertwined.

In this work, we present a microscopic theory of the inverse chiral phonon Zeeman effect based on dynamical piezoelectricity within the framework of micropolar elasticity [20, 21]. Focusing on chiral phonons propagating with non-zero wave number along a screw axis, we show that intrinsic lattice dynamics generates an internal elliptically polarized magnetic field, establishing a purely lattice-driven route to magnetoelectric coupling. In particular, we show that chiral lattice dynamics alone generates an effective longitudinal Zeeman field acting on electronic spins, without invoking external light or static magnetic fields.

*Model.* We consider a noncentrosymmetric crystal whose elastic properties are described by the theory of micropolar elasticity. In this framework, translational polar displacements  $\mathbf{u}(\mathbf{r})$  and axial microrotations  $\varphi(\mathbf{r})$  at position  $\mathbf{r}$  are treated as independent but dynamically coupled fields [20–22]. The strain (Cauchy) and wryness (Cosserat) tensors are defined as  $\varepsilon_{kl} = \partial_l u_k - \epsilon_{klm} \varphi_m$  and  $\gamma_{kl} = \partial_l \varphi_k$ , respectively. Here,  $\epsilon_{klm}$  is the Levi-Civita symbol.

For definiteness and following our previous work [22], we consider a crystal with a hexagonal space group  $P6_322$

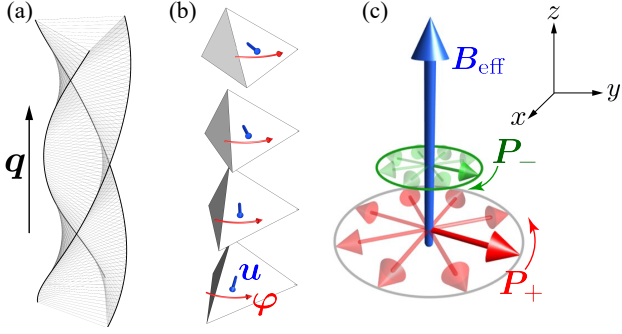


FIG. 1. (Color online) Schematic illustration of (a) a chiral elastic wave in a continuum description, (b) independent translational and rotational degrees of freedom of rigid blocks, which constitute the basic viewpoint of micropolar elasticity, and (c) an effective longitudinal magnetic field induced by lifting the degeneracy of counter-rotating piezoelectric waves.

and analyze plane-wave solutions propagating along the chiral  $z$  axis [see Fig. 1(a) and (b)].

The Lagrangian density for the transverse components  $u_i$  and  $\varphi_i$  ( $i = 1$  and  $2$  correspond to  $x$  and  $y$ , respectively) reads as

$$\mathcal{L}_T = \frac{\rho}{2} \dot{u}_i^2 - \frac{A_{55}}{2} (\partial_z u_i)^2 + \frac{\rho j_1}{2} \dot{\varphi}_i^2 - \frac{B_{44}}{2} (\partial_z \varphi_i)^2 - \frac{1}{2} (A_{44} - 2A_{47} + A_{55}) \varphi_i^2 + (A_{47} - A_{55}) \epsilon_{ij} u_i \partial_z \varphi_j - C_{74} \partial_z \varphi_i \partial_z u_i + (C_{44} - C_{74}) \epsilon_{ij} \varphi_i \partial_z \varphi_j, \quad (1)$$

where  $\rho$  is the mass density and  $j_1$  is the microinertia associated with lattice rotations,  $\epsilon_{ij}$  is the 2-dimensional Levi-Civita symbol. The components  $A_{ij}$ ,  $B_{ij}$  and  $C_{ij}$  of the even-rank polar tensors and the pseudotensor, respectively, are written in the generalized Voigt (Sirotin) notation [23]. The chiral coupling terms with  $C_{ij}$  lift the degeneracy between right- and left-handed phonon modes even in the absence of any magnetic or optical pumping field [22].

Canonical quantization of the transverse modes and diagonalization using the Bogoliubov  $uv$ -transformation yields the Hamiltonian (see Sec. I in Ref. [24])

$$\hat{H}_T = \Delta E_0^{(T)} + \sum_{q,s} \left[ \hbar \omega_{sq}^{(A)} \hat{\alpha}_{s,q}^\dagger \hat{\alpha}_{s,q} + \hbar \omega_{sq}^{(O)} \hat{\beta}_{s,q}^\dagger \hat{\beta}_{s,q} \right], \quad (2)$$

where  $\Delta E_0^{(T)}$  is a correction term of the vacuum energy,  $s = \pm$  labels the circular polarization (right- or left-handed), and  $\hat{\alpha}_{s,q}$  and  $\hat{\beta}_{s,q}$  are the annihilation operators for the acoustic and optical branches, respectively, with the wave-vector  $q = (0, 0, q)$  [see Fig. 1(a)]. The corresponding dispersion relations  $\omega_{sq}^{(A/O)}$  coincide with those of the classical theory [22].

A similar analysis can be carried out for longitudinal micropolar elastic waves propagating along the  $z$  direction. Since the inverse chiral phonon Zeeman mechanism

discussed below is governed by circularly polarized transverse modes, the longitudinal modes play no essential role in the following and will be neglected.

*Magnetic fields induced by dynamical piezoelectric waves.* In a piezoelectric micropolar medium, elastic waves are accompanied by a time-dependent electric polarization  $\mathbf{P}$ . In centrosymmetric crystals, such polarization dynamics induces magnetization in the form  $\mathbf{M} \sim \mathbf{P} \times \partial_t \mathbf{P}$ , which reflects the collective circular motion of ions [3]. In contrast, as we will show below, in the noncentrosymmetric setting the dynamical piezoelectric coupling generates internal circularly polarized *magnetic fields* that interact directly with electronic spins.

From the constitutive relation of the micropolar medium [21] with the point group 622 (see Sec. II in Ref. [24]), the transverse components  $u_\pm = u_1 \pm i u_2$  and  $\varphi_\pm = \varphi_1 \pm i \varphi_2$  determine the decoupled circularly polarized modes of the electric polarization,  $P_\pm = P_1 \pm i P_2$ , in the form

$$P_\pm(q, t) = \pm q \left( d_{14} + \frac{1}{2} X_{11} \right) u_\pm(q, t) + \left( X_{11} \mp q \Gamma_{11}^{(1)} \right) \varphi_\pm(q, t). \quad (3)$$

Here,  $d_{14}$ , and  $X_{11}$ ,  $\Gamma_{11}^{(1)}$  are the components of the conventional piezoelectric tensor and two additional tensors related to the rotational degrees of freedom, respectively. The longitudinal polarization  $P_3$  does not contribute to the mechanism discussed below.

The magnetic field associated with the polarization dynamics follows from the Maxwell–Ampère equation for nonmagnetic media,  $\nabla \times \mathbf{B} = \mu_0 \partial_t \mathbf{P}$ . For the circularly polarized magnetic components it takes the form [see Fig. 1(c)]

$$B_\pm(q, t) = \mp \frac{\mu_0}{q} \partial_t P_\pm(q, t). \quad (4)$$

Upon canonical quantization of the displacement and rotation fields, one obtains the magnetic-field operators  $\hat{B}_{\pm,q}(t)$ , satisfying  $\hat{B}_{\pm,q}^\dagger(t) = \hat{B}_{\mp,-q}(t)$  [24]. The single-phonon magnetic-field states  $|B_{\pm,q}\rangle = \hat{B}_{\pm,q}^\dagger |0\rangle$  define the intrinsic magnetic-field scale associated with a *single quantum* of a chiral phonon mode.

The inner product of the single phonon magnetic-field states takes the form

$$\langle B_{\pm,q} | B_{\pm,q} \rangle = \frac{\hbar \mu_0^2}{2 \rho V_0 q^2} \sum_{s=A,O} \left[ \omega_{\pm q}^{(s)} \right]^2 \mathcal{F}_{\pm}^{(s)}(q), \quad (5)$$

where the explicit expression  $\mathcal{F}_{\pm}^{(s)}(q)$  is given in Supplementary Materials (Sec. II). Importantly, Eq. (5) is time independent and defines the *single-phonon rms magnetic-field amplitude*  $B_\pm^{(1)}(q) \equiv \sqrt{\langle B_{\pm,q} | B_{\pm,q} \rangle}$ .

Figure 2 shows the resulting wave-number dependence of  $B_\pm^{(1)}(q)$ . The asymmetry between the two circular polarizations,  $B_+^{(1)}(q) \neq B_-^{(1)}(q)$ , is a direct consequence of

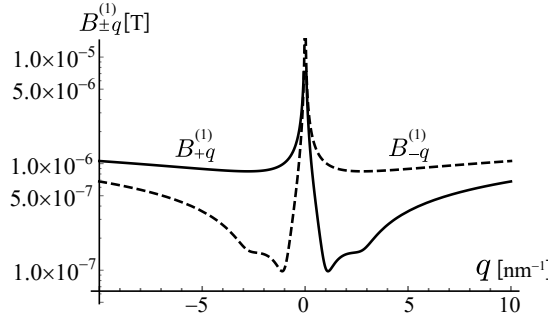


FIG. 2. (Color online) Calculated single-phonon magnetic-field amplitudes  $B_{\pm}^{(1)}(q)$  as a function of phonon wave number  $q$ . Material parameters are taken from Ref. [22]; see text for details.

broken inversion symmetry and implies that electrons experience an elliptically polarized internal magnetic field. In the long-wavelength limit  $q \rightarrow 0$ , the dominant contribution originates from the gapped rotational modes with frequencies  $\omega_{\pm q}^{(O)}$ , which play a role analogous to IR-active optical modes in centrosymmetric crystals [1], but without requiring any external perturbation to lift their degeneracy.

*Many-phonon enhancement.* Once the magnetic field associated with a single phonon quantum is established, the enhancement in coherent phonon states follows naturally and can be discussed in a controlled and quantitative manner.

Equation (5) and Fig. 2 quantify the magnetic-field scale associated with a *single* phonon quantum. In nonequilibrium situations, however, the relevant chiral phonon mode may acquire a macroscopic occupation. For a mode with occupation number  $N_{\pm}(q)$ , the cycle-averaged field intensity scales as  $\langle B_{\pm}^2(q) \rangle \propto [2N_{\pm}(q) + 1] [B_{\pm}^{(1)}(q)]^2$ , so that the rms magnetic-field amplitude grows as  $B_{\pm}^{\text{rms}}(q) \sim \sqrt{2N_{\pm}(q) + 1} B_{\pm}^{(1)}(q)$ . In particular, a coherent phonon state yields a classical magnetic-field component with amplitude  $\propto \sqrt{N_{\pm}}$ , providing a natural route to amplify the internal magnetic field by orders of magnitude relative to the single-phonon scale.

*Zilch and phonon-induced magnetic chirality.* The elliptically polarized magnetic field generated by a dynamical piezoelectric wave carries an intrinsic measure of magnetic chirality. The latter can be characterized by Lipkin's Zilch density [25],

$$Z(\mathbf{r}, t) = \mathbf{B}(\mathbf{r}, t) \cdot [\nabla \times \mathbf{B}(\mathbf{r}, t)], \quad (6)$$

which provides a gauge-invariant measure of optical and magnetic chirality.

Making Fourier transformation,  $Z(z, t) = \int (dq/2\pi) Z_q(t) e^{iqz}$ , and using quantization of the magnetic field and polarization in terms of phonon

operators, the expectation value of the Zilch density in the phonon vacuum becomes time independent (see Sec. III in Ref.[24]),

$$\langle \hat{Z}_q \rangle = -\frac{\delta_{q,0}}{4\pi\hbar} \int dk k (\langle B_{+,k} | B_{+,k} \rangle - \langle B_{-,k} | B_{-,k} \rangle). \quad (7)$$

Hence, a nonzero Zilch directly reflects the intrinsic asymmetry between the counter-rotating magnetic components,  $\langle B_{+,k} | B_{+,k} \rangle \neq \langle B_{-,k} | B_{-,k} \rangle$ , which originates from the chiral splitting of the underlying phonon modes. This result establishes that the dynamical piezoelectric waves generate not only an internal magnetic field, but also a finite magnetic chirality rooted in lattice symmetry.

*Phonon-induced electron spin polarization.* The elliptically polarized magnetic field  $\mathbf{B}(t)$  generated by the dynamical piezoelectric wave acts on electronic spins as an effective ac Zeeman field. In this work, electrons are treated as passive probes of the phonon-induced magnetic field.

We consider the Hamiltonian of a single-electron spin  $\boldsymbol{\sigma}$  coupled to the counter-rotating magnetic field components,

$$\hat{H}(t) = \mu_B \boldsymbol{\sigma} \cdot \mathbf{B}_+(t) + \mu_B \boldsymbol{\sigma} \cdot \mathbf{B}_-(t), \quad (8)$$

where  $\mu_B$  is the Bohr magneton and  $\mathbf{B}_{\pm}(t)$  represent clockwise and anticlockwise rotating magnetic fields with the frequencies  $\omega_{\pm} = \omega_{\pm q}^{(O)}$ . The two frequencies are nearly degenerate,  $|\omega_+ - \omega_-| \ll \omega = (\omega_+ + \omega_-)/2$ , while the amplitudes generally differ due to lattice chirality,  $B_+ \neq B_-$ .

When the typical electronic energy scale is smaller than or comparable to  $\hbar\omega_{\pm}$ , the time-periodic Hamiltonian (8) can be treated within the Floquet high-frequency expansion [26–30]. To leading order, this yields the effective static Floquet Hamiltonian [31, 32] (see Sec. IV in Ref. [24]),

$$\hat{H}_{\text{eff}} \simeq -2 \frac{\mu_B^2}{\hbar\omega} (B_+^2 - B_-^2) \sigma_z, \quad (9)$$

which describes an emergent Zeeman field along the  $z$  axis. The effective field is proportional to the *intensity difference* of the counter-rotating magnetic components, reflecting the phonon-induced magnetic chirality.

Unlike optically driven magnetization [5, 33], the present effect originates intrinsically from the internal lattice dynamics, without any external light or static magnetic field. While this statement concerns the microscopic mechanism, the magnitude of the emergent Zeeman field is controlled by the occupation of the underlying chiral phonon modes.

Since the Floquet-induced static Zeeman term depends on the intensity difference, one finds

$$B_{\text{eff}} \propto \frac{N_+(q)}{\omega} [B_+^{(1)}(q)]^2 - \frac{N_-(q)}{\omega} [B_-^{(1)}(q)]^2, \quad (10)$$

where  $B_{\pm}^{(1)}(q)$  denote the single-phonon magnetic-field amplitudes. Hence, in a coherent phonon state or a strongly populated nonequilibrium regime, the effective Zeeman field increases *linearly* with the phonon occupation.

*Inverse Zeeman phonon splitting effect.* The phonon-induced elliptically polarized magnetic field gives rise to a spin-dependent modification of the electronic spectrum. At this stage, the role of electrons is purely passive: the electronic system responds to the effective Zeeman field generated by chiral phonons, without feeding back onto the lattice dynamics.

The coupling between conduction electrons and the circularly polarized magnetic components can be described by the interaction Hamiltonian

$$\mathcal{H}_{\text{int}} = -\frac{1}{2}g_e\mu_B \sum_{\mathbf{k},\mathbf{q}} \left[ B_{-}(\mathbf{q}) c_{\mathbf{k}+\mathbf{q}\uparrow}^{\dagger} c_{\mathbf{k}\downarrow} + B_{+}(\mathbf{q}) c_{\mathbf{k}+\mathbf{q}\downarrow}^{\dagger} c_{\mathbf{k}\uparrow} \right], \quad (11)$$

where  $g_e$  is the electron  $g$  factor,  $c_{\mathbf{k}\sigma}^{\dagger}$  ( $c_{\mathbf{k}\sigma}$ ) are the electron creation (annihilation) operators in the state  $\mathbf{k}\sigma$  ( $\sigma = \uparrow, \downarrow$ ). This interaction has the same structure as a Zeeman coupling to a circularly polarized magnetic field, with the crucial difference that the field here is generated internally by lattice dynamics. The inequivalence  $|B_{+}| \neq |B_{-}|$ , originating from the chiral splitting of the phonon modes, produces a Zeeman-like spin-dependent band splitting (see Sec. V in Ref. [24]).

To obtain the concomitant net magnetization,  $\langle m_z \rangle$ , we focus on a single phonon wave vector  $\mathbf{Q} = (0, 0, Q)$ . For the case of weak splitting,  $|B_{+}(\mathbf{Q})|^2 - |B_{-}(\mathbf{Q})|^2 \ll \varepsilon_F^2$  ( $\varepsilon_F$  is the Fermi energy),  $\langle m_z \rangle$  can be obtained perturbatively. Assuming that only the lower quasiparticle branches are occupied, one gets

$$\langle m_z \rangle \approx \frac{1}{8} (g_e\mu_B)^3 S(\mathbf{Q}) (|B_{+}(\mathbf{Q})|^2 - |B_{-}(\mathbf{Q})|^2), \quad (12)$$

where the dimensionless factor  $S(\mathbf{Q})$ , defined in the Supplementary Materials, encodes the electronic density of states and kinematic details. Eq. (12) explicitly shows that the phonon chirality controls the induced electronic magnetization.

Here we note that Eq. (12) does not take into account the breaking of inversion symmetry in the electronic system. In noncentrosymmetric crystals, however, the bulk Rashba effect is allowed. It can be shown that weak Rashba splitting leads to second-order corrections with respect to the Rashba constant for the electronic net magnetization (see Sec. VI in Ref. [24]).

*Validity of the piezoelectric scenario.* A key requirement for the dynamical piezoelectric mechanism is that the induced polarization is not efficiently screened by conduction electrons. This imposes the condition that the characteristic phonon frequency  $\omega$  should be comparable to or exceed the electronic plasma frequency  $\omega_p$ .

For a free-electron gas,  $\omega_p \simeq 56.4\sqrt{n}$  Hz, so that for optical phonon frequencies in the range 6–12 THz the condition  $\omega \gtrsim \omega_p$  is satisfied for carrier densities below  $n \sim 10^{23}$  m<sup>-3</sup>. The present theory therefore naturally applies to piezoelectric insulators and lightly doped semiconductors, where electronic screening is incomplete.

This frequency hierarchy also justifies the use of the Floquet high-frequency expansion employed in our analysis. When the phonon frequency exceeds the relevant electronic energy scales, the time-periodic Zeeman coupling generated by the lattice dynamics can be replaced by an effective static Hamiltonian without loss of accuracy. Thus, the same condition that suppresses electronic screening simultaneously ensures the internal consistency of the Floquet description.

*Coherent-phonon and selective excitation of a target wave vector.* The inverse chiral phonon Zeeman effect discussed in this work is governed predominantly by the occupation of a *specific* chiral phonon mode with a well-defined wavenumber  $q = Q$  along the rotational axis. Therefore, the ability to selectively exciting and coherently controlling a target phonon wavenumber provides a direct experimental handle to tune both the magnitude and the sign of the induced Zeeman field. In practice, such mode selectivity is most naturally achieved by preparing the phonon mode in a coherent state, which simultaneously allows one to address a single wave vector and to enhance the magnetic-field amplitude.

For the single circularly polarized phonon mode, we consider a coherent phonon state

$$|\alpha_{\pm}(q)\rangle = \exp\left(-\frac{1}{2}|\alpha_{\pm}|^2\right) \sum_{n=0}^{\infty} \frac{\alpha_{\pm}^n}{\sqrt{n!}} |n_{\pm}(q)\rangle, \quad (13)$$

which satisfies  $\langle \alpha_{\pm} | \hat{a}_{\pm,q}^{\dagger} \hat{a}_{\pm,q} | \alpha_{\pm} \rangle = N_{\pm}(q) = |\alpha_{\pm}|^2$ . In such a state, the expectation value of the lattice displacement acquires a classical amplitude  $u_0$ , providing a direct link between the coherent excitation and the phonon occupation number.

Using the material parameters adopted in Fig. 2, the phonon occupation associated with a coherently excited elastic wave can be estimated directly from the lattice displacement amplitude. Specifically, the occupation number is related to  $u_0$  as  $N_{\pm}(q) \simeq (u_0/2u_{\text{zp}})^2$ , with  $u_{\text{zp}} = \sqrt{\hbar/2\rho V_0 \omega}$ , where  $u_{\text{zp}}$  is the zero-point displacement,  $\rho$  is the mass density,  $V_0$  is the unit cell volume, and  $\omega$  is the phonon frequency. With the parameters used in Fig. 2 [24] and a typical optical-phonon frequency  $\omega/2\pi \sim 10$  THz, one finds  $u_{\text{zp}} \sim 6 \times 10^{-13}$  m  $\approx 0.006$  Å. Consequently, an Å-scale coherent lattice displacement, which may correspond to the upper bound of physically reasonable amplitudes, leads to an occupation number at most of the order of  $N_{\pm} \sim (u_0/2u_{\text{zp}})^2 \sim 10^4$ .

Since the Floquet-induced static Zeeman field scales linearly with the phonon occupation number,  $B_{\text{eff}} \propto N_{+}(q) - N_{-}(q)$ , the use of a coherent phonon state target-

ing a specific wave vector  $q = Q$  implies that the effective Zeeman field can be enhanced by up to  $\sim 10^4$  compared to the single-phonon scale. The ultimate magnitude of the effect is limited by anharmonicity, damping, and, in conducting systems, residual electronic screening.

To facilitate comparison with experimentally reported phonon magnetic moments, which are often quoted in units of the Bohr magneton  $\mu_B$ , it is convenient to convert the internal magnetic-field scale into an equivalent magnetic moment per unit cell. Identifying the magnetization as  $M = B/\mu_0$ , we define  $\mu_{\text{cell}}(q) \equiv M(q)V_0 = (V_0/\mu_0)B(q)$ , and  $\mu_{\text{cell}}(q)/\mu_B = (V_0/\mu_0\mu_B)B(q)$ . For the unit-cell volume  $V_0 = 3.988 \times 10^{-28} \text{ m}^3$  used throughout this work, this relation yields  $\mu_{\text{cell}}/\mu_B \simeq 34.2 \times B[\text{T}]$ , providing a direct correspondence between the internal magnetic-field amplitude and the effective phonon magnetic moment.

Finally, we note that selectively addressing a target wave vector  $\mathbf{Q}$  can be realized by a momentum-selective drive—for example, a transient-grating setup that defines  $\mathbf{Q}$  or a patterned electromechanical transducer that launches a piezoelectric wave with  $q = Q$  along the chiral axis. In this language, the driven chiral mode is prepared in a coherent state  $|\alpha_{\pm}(\mathbf{Q})\rangle$  with  $\langle \hat{a}_{\pm, \mathbf{Q}} \rangle = \alpha_{\pm}$  and  $N_{\pm} = |\alpha_{\pm}|^2$ , so that the Floquet Zeeman field is directly tunable through the helicity imbalance of the coherently populated mode [see Eq. (10) for  $B_{\text{eff}}$  above].

In summary, we have demonstrated that chiral lattice dynamics in noncentrosymmetric crystals generate an internal magnetic field through dynamical piezoelectricity, even in the absence of external light or static magnetic fields. Within a microscopic description based on micropolar elasticity, this field acts as an effective longitudinal Zeeman field on electronic spins in the high-frequency Floquet regime, provided that electronic screening is incomplete. The resulting inverse chiral phonon Zeeman effect establishes a lattice-driven mechanism for spin polarization and spin-dependent band splitting, and provides a route to controlling magnetoelectric responses via chiral phonons.

J.K. acknowledges support from JSPS KAKENHI Grant Nos. JP25K00962, JP25H02149, and JP23H00091, and from the OML Project grant by the National Institutes of Natural Sciences (NINS program No. OML012301). A.S.O. thanks the Ministry of Science and Higher Education of the Russian Federation (FEUZ 2023-0017). M.S. acknowledges support from JSPS KAKENHI Grant Nos. JP25K07198, JP25H02112, JP22H05131, JP25H01609, and JP25H01251, JST CREST (Grant No. JPMJCR24R5), and the JSPS Program for Forming J-PEAKS (Grant No. JPJS00420230002).

---

- [1] G. Schaack, Solid State Communications **17**, 505 (1975).
- [2] G. Schaack, Journal of Physics C: Solid State Physics **9**, L297 (1976).
- [3] D. M. Juraschek, M. Fechner, A. V. Balatsky, and N. A. Spaldin, Phys. Rev. Mater. **1**, 014401 (2017).
- [4] D. M. Juraschek and N. A. Spaldin, Phys. Rev. Mater. **3**, 064405 (2019).
- [5] D. M. Juraschek, P. Narang, and N. A. Spaldin, Phys. Rev. Res. **2**, 043035 (2020).
- [6] R. M. Geilhufe, V. Jüri, S. Bonetti, J.-X. Zhu, and A. V. Balatsky, Physical Review Research **3**, L022011 (2021).
- [7] S. Chaudhary, D. M. Juraschek, M. Rodriguez-Vega, and G. A. Fiete, Physical Review B **110**, 094401 (2024).
- [8] N. Shabala, F. Tietjen, and R. M. Geilhufe, arXiv:2511.03329 (2025).
- [9] B. Cheng, T. Schumann, Y. Wang, X. Zhang, D. Barbalas, S. Stemmer, and N. P. Armitage, Nano Letters **20**, 5991 (2020).
- [10] A. Baydin *et al.*, Physical Review Letters **128**, 075901 (2022).
- [11] F. Wu, S. Bao, J. Zhou, Y. Wang, J. Sun, J. Wen, Y. Wan, and Q. Zhang, Nature Physics **19**, 1868 (2023).
- [12] F. G. Hernandez *et al.*, Science Advances **9**, eadj4074 (2023).
- [13] R. M. Geilhufe, Phys. Rev. Res. **4**, L012004 (2022).
- [14] J. Fransson, Physical Review Research **5**, L022039 (2023).
- [15] N. Shabala and R. M. Geilhufe, Physical Review Letters **133**, 266702 (2024).
- [16] L. Klebl, A. Schobert, M. Eckstein, G. Sangiovanni, A. V. Balatsky, and T. O. Wehling, Phys. Rev. Lett. **134**, 016705 (2025).
- [17] R. Merlin, Physical Review B **110**, 094312 (2024).
- [18] R. Merlin, PNAS Nexus **4**, pgaf002 (2025).
- [19] K. Ishito, H. Mao, Y. Kousaka, Y. Togawa, S. Iwasaki, T. Zhang, S. Murakami, J.-i. Kishine, and T. Satoh, Nature Physics **19**, 35 (2023).
- [20] A. C. Eringen, *Microcontinuum Field Theories: I. Foundations and Solids* (Springer, New York, 1999).
- [21] W. Nowacki, *Theory of Asymmetric Elasticity* (Pergamon Press, Oxford, 1986).
- [22] J.-i. Kishine, A. S. Ovchinnikov, and A. A. Tereshchenko, Physical Review Letters **125**, 245302 (2020).
- [23] Y. I. Sirotin and M. P. Shaskolskaya, *Fundamentals of Crystal Physics* (Mir Publishers, Moscow, 1982).
- [24] See supplemental material, <https://link.aps.org/supplemental/PRL/XX/XXXXXX>, for details of the derivations, dispersion relations, and additional numerical results.
- [25] D. M. Lipkin, Journal of Mathematical Physics **5**, 696 (1964).
- [26] M. Bukov, L. D'Alessio, and A. Polkovnikov, Advances in Physics **64**, 139 (2015).
- [27] A. Eckardt and E. Anisimovas, New J. Phys. **17**, 093039 (2015), doi:10.1088/1367-2630/17/9/093039.
- [28] A. Eckardt, Rev. Mod. Phys. **89**, 011004 (2017), doi:10.1103/RevModPhys.89.011004.
- [29] T. Oka and S. Kitamura, Annu. Rev. Condens. Matter Phys. **10**, 387 (2019), doi:10.1146/annurev-conmatphys-031218-013423.
- [30] M. Sato and T. N. Ikeda, J. Phys. Soc. Jpn. **94**, 111007

(2025).

[31] S. Takayoshi, M. Sato, and T. Oka, Phys. Rev. B **90**, 214413 (2014), doi:10.1103/PhysRevB.90.214413.

[32] M. Sato, S. Takayoshi, and T. Oka, Phys. Rev. Lett. **117**, 147202 (2016), doi:10.1103/PhysRevLett.117.147202.

[33] H. Ishizuka and M. Sato, arXiv:2505.05313 (2025).